Unsteady Turbulence Measurements in Breaking Tidal Bores including the Effect of Bed Roughness

N.J. Docherty[1] and H. Chanson[1]
[1]School of Civil Engineering
The University of Queensland
Brisbane QLD 4072
AUSTRALIA
E-mail: h.chanson@uq.edu.au

Abstract: *A tidal bore is an unsteady flow motion generated by the rapid water level rise at the river mouth during the early flood tide under appropriate macro-tidal and bathymetric conditions. The present study investigated physically the turbulent properties of breaking tidal bores. The results were based upon some experimental measurements of free-surface fluctuations and turbulent velocities conducted on smooth and rough beds. Using an ensemble-averaging technique, the free-surface fluctuations of breaking tidal bores were characterised. Immediately prior to the roller, the free-surface curved gradually upwards, and the passage of the bore roller was associated with some large water elevation fluctuations. The turbulent velocity measurements were performed at several vertical elevations during the breaking bore. Both the instantaneous and ensemble-averaged velocity data highlighted some strong flow deceleration at all elevations. Close to the bed, the longitudinal velocity component became negative immediately after the roller indicating the existence of a transient recirculation. The vertical velocity data presented some positive, upward motion beneath the roller with increasing maximum vertical velocity at increasing elevation above the bed. The transverse velocity data show some large fluctuations with a non-zero ensemble-average after the roller passage, suggesting some secondary turbulent motion advected behind the bore.*

Keywords: *Tidal bores, Breaking roller, Physical modelling, Bed roughness, Turbulence, Ensemble-average.*

1. INTRODUCTION

A tidal bore is an unsteady open channel flow generated by the rapid water level rise at the river mouth during the early flood tide. The development of the bore is closely linked with macro-tidal conditions, a funnel-shaped estuary and relatively low freshwater levels to satisfy some momentum considerations. With time, the leading edge of the tidal wave becomes steeper until it forms a wall of water: i.e., the tidal bore. After the formation of the bore, there is a discontinuity in water depth and velocity field at the bore front (Fig. 1). Once formed, the flow properties immediately before and after the tidal bore must satisfy the equations of conservation of mass and momentum (Rayleigh 1908, Henderson 1966, Liggett 1994).

Despite some recent advances, the unsteady turbulent motion in a tidal bore remains poorly understood. In the present study, the turbulent flow properties of breaking tidal bores were investigated physically under well-controlled flow conditions. The analysis was based upon some experimental measurements of free-surface fluctuations and turbulent velocities conducted in a relatively large facility on smooth and rough beds. It is the aim of this study to characterise the unsteady turbulent mixing in breaking tidal bores.

Figure 1 Breaking tidal bore of the Sélune River in Bay of Mont Saint Michel (France) on 24 September 2010 - Bore propagation from left to right

1.1. Physical modelling of tidal bores

The laboratory studies of tidal bores are performed with geometrically similar models. The physical modelling requires the selection of an adequate similitude. For a tidal bore, the theoretical considerations show that the relevant characteristic length and velocity scales are respectively the initial flow depth d_o and initial relative velocity (V_o+U), where V_o is the initial flow velocity positive downstream and U is the bore celerity positive upstream (Henderson 1966, Liggett 1994). For a tidal bore propagating in a horizontal, rectangular channel, a simplified dimensional analysis yields:

$$\frac{d}{d_o}, \frac{V_x}{V_o}, \frac{V_y}{V_o}, \frac{V_z}{V_o} = F\left(\frac{x}{d_o}, \frac{y}{d_o}, \frac{z}{d_o}, t\sqrt{\frac{g}{d_o}}, \frac{V_o + U}{\sqrt{g d_o}}, \rho \times \frac{(V_o + U) d_o}{\mu}, \frac{\delta}{d_o}, \frac{B}{d_o}, \frac{g \mu^4}{\rho \sigma^3}, ...\right) \quad (1)$$

where d is the flow depth, V_x, V_y, V_z are respectively the longitudinal, transverse and vertical velocity components at a location (x, y, z), x is the coordinate in the flow direction, y is the horizontal transverse coordinate measured from the channel centreline, z is the vertical coordinate measured from channel bed, t is the time, δ is the initial boundary layer thickness at x, B is the channel width, g is the gravity acceleration, ρ and μ are the water density and dynamic viscosity respectively, and σ is the surface tension between air and water. Equation (1) expresses the dimensionless unsteady flow properties (left handside terms) at a position (x, y, z) and at a time t as functions of the dimensionless tidal bore properties, initial flow properties, channel geometry and fluid properties. In the right handside, the fifth and sixth terms are the tidal bore Froude and Reynolds numbers respectively, and the ninth term is the Morton number which is a function of fluid properties and gravity constant only.

In free-surface flows including tidal bores, the gravity effects are important and a Froude similitude is commonly used (Henderson 1966, Chanson 1999). But the turbulent mixing processes are dominated by viscous forces implying the needs for a Reynolds similarity. Figure 1 illustrates indeed the turbulence of a breaking tidal bore front. For geometrically-similar tidal bore models, it is impossible to satisfy simultaneously all the similarities because of too many relevant parameters (Eq. (1)). In practice, the physical studies are based upon a Froude similitude, but no systematic study has been conducted to date to ascertain any scale effect affecting the turbulent mixing in tidal bore flows.

2. EXPERIMENTAL FACILITY AND INSTRUMENTATION

The experiments were performed in a 12 m long, 0.5 m wide tilting flume (Docherty and Chanson 2010). The channel was made of smooth PVC bed and glass walls. The water was supplied by a constant head tank, and a fast-closing gate was located at the channel downstream end. Two channel bed roughnesses were tested. A series of experiments was conducted on the smooth PVC invert. For the second series of experiments, the bed was covered with plywood sheets covered by natural blue granite gravels sieved between 4.75 mm and 6.70 mm, glued in resin and covered by a spray gloss surface finish. The hydraulic roughness of the gravel bed was tested. The equivalent Darcy friction factor was f = 0.036 on average, and the equivalent sand roughness height was k_s = 3.4 mm.

The steady flow rate was measured with two orifice meters that were calibrated on site. The water depths were measured using rail mounted pointer gauges in steady flows. In unsteady flows, the water depths were recorded using a number of acoustic displacement meters (Microsonic™ Mic+25/IU/TC) located among the channel. The turbulent velocity measurements were performed with a Nortek™ Vectrino+ acoustic Doppler velocimeter (ADV) equipped with a side-looking head (Fig. 2). The velocity range was set to 1.0 m/s, and the data accuracy was 0.01 m/s. The translation of the ADV probe in the vertical direction was controlled by a fine adjustment travelling mechanism with an error less than 0.1 mm. Herein the measurements were performed on the channel centreline, and the ADV and displacement sensors were synchronised and sampled simultaneously at 200 Hz. Further information on the experimental apparatus was reported in Docherty and Chanson (2010).

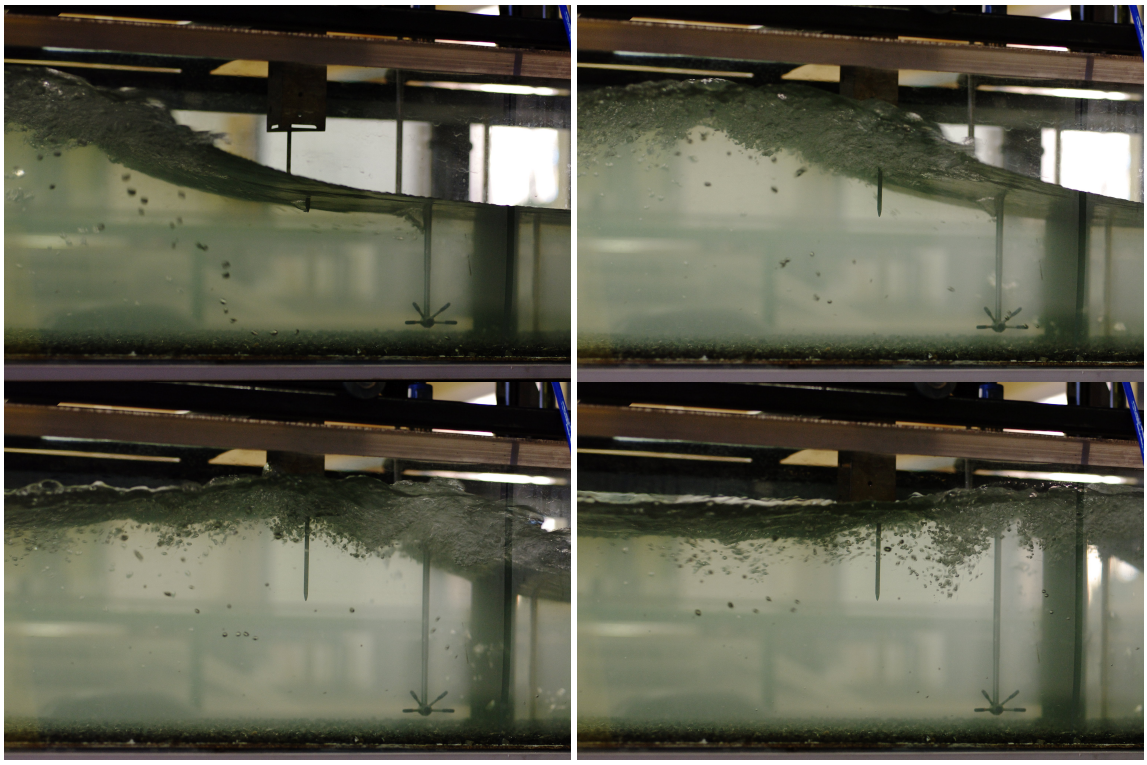

Figure 2 Breaking bore propagation (from left to right): d_o = 0.125 m, Fr = 1.5, Re = 1.9×10^5, fixed gravel bed, shutter: 1/100 s, continuous shooting at 5.2 fps (from left to right, top to bottom) - Note the ADV head on the right

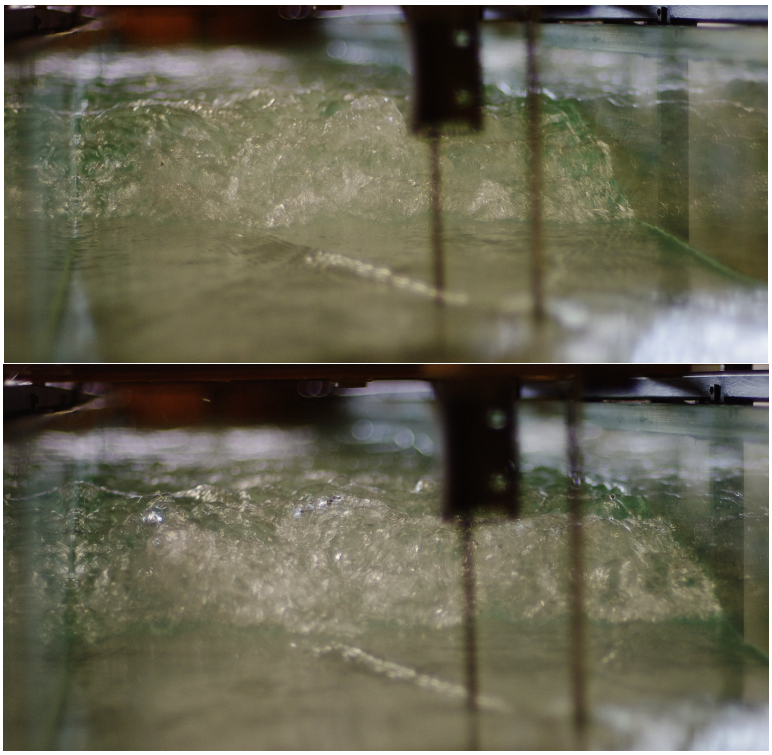

Figure 3 Breaking bore propagation (from background to foreground) looking downstream: d_o = 0.116 m, Fr = 1.6, Re = 2×10^5, smooth PVC bed, shutter: 1/100 s, continuous shooting at 5.2 fps

2.1. INFLOW CONDITIONS AND TIDAL BORE GENERATION

For each experimental run, the steady gradually-varied flow conditions were established for 5 minutes prior to the first measurements. The tidal bore was generated by the rapid partial closure of the downstream gate. The gate closure time was less than 0.15 s. After closure, the bore propagated upstream (Fig. 2 & 3) and each experiment was stopped before the bore front reached the channel upstream end to avoid any wave reflection effect. The ADV measurements were conducted at x = 5 m downstream of the channel upstream end. Some detailed steady flow measurements showed that the boundary layer was partially-developed at x = 5 m: δ/d_o = 0.47 and 0.64 for smooth bed and fixed gravel bed respectively.

The free-surface properties were documented for tidal bore Froude numbers between 1.01 and 1.65. The velocity measurements were conducted in breaking bores for $0.005 < z/d_o < 0.77$, where z was measured above the top of the gravel material using a semi-circular footing of 25.1 cm^2 area. At a number of vertical elevations, a series of twenty instantaneous velocity records were repeated with the same well-defined initially-steady flow conditions, and an ensemble-median of each instantaneous velocity component was calculated.

3. BASIC FLOW PATTERNS

The free-surface observations highlighted two types of tidal bores depending upon the Froude number. For a Froude number between unity and 1.5, the tidal bore was undular. The bore consisted of first wave followed by a train of well-formed undulations. The wave steepness data showed a monotonic increase with an increasing Froude number for $1 < Fr < 1.35$, then a local maximum for Fr = 1.35 to 1.4, followed by a sharp decrease immediately before the disappearance of free-surface undulations. The observations were identical for smooth and rough bed, and consistent with a number of data sets (Koch and Chanson 2009, Chanson 2010).

For large Froude numbers (Fr > 1.5), a breaking bore with a marked roller was observed (Fig. 2 & 3). For a tidal bore with a marked roller (Fr = 1.5-1.6), the free-surface properties were systematically investigated by repeating 25 identical experiments and the results were ensemble-averaged. An example is shown in Figure 4. Figure 4 present the time-variations of the ensemble-averaged median water depth and fluctuations for smooth PVC bed. Each graph includes the ensemble-averaged median water depth d_{median}, and the differences between 3rd and 4th quartiles (d_{75}-d_{25}) and 90% and 10% percentiles (d_{90}-d_{10}), and the difference between maximum and minimum depths (d_{max}-d_{min}). Here (d_{75}-d_{25}), (d_{90}-d_{10}) and (d_{max}-d_{min}) characterised the free-surface fluctuations around the median value.

Both the free-surface measurements and the visual observations showed that the free-surface elevation rose first slowly by about $0.1d_o$, immediately prior to the roller (Fig. 4). Such a gradual rise in free-surface ahead of the turbulent roller was previously observed by Hornung et al. (1995) and Koch and Chanson (2009). Immediately after, the turbulent roller caused by a sharp rise in water depth (Fig. 4). Further the free-surface fluctuations were the largest next to the roller toe and impingement point, and they decayed quasi-exponentially with increasing time as the bore roller passed beneath the sensor. Typically the maximum free-surface fluctuations were observed during the first half of the bore roller for both smooth and rough bed (Fig. 4).

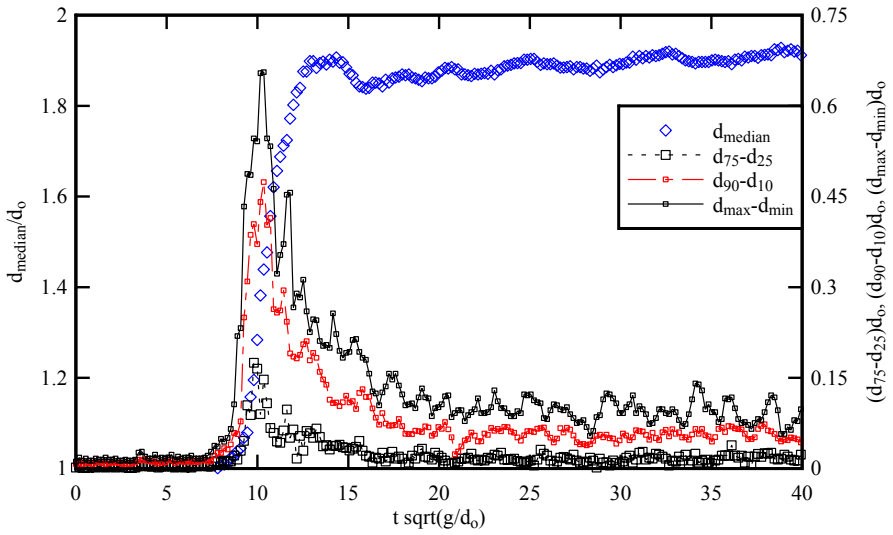

Figure 4 Ensemble-average median water depth d_{median}, difference between 3rd and 4th quartiles (d_{75}-d_{25}) and 90% and 10% percentiles (d_{90}-d_{10}), and range of maximum to minimum water depths (d_{max}-d_{min}) in a breaking tidal bore: Fr = 1.66, Re = 2.1×10^5, Q = 0.050 m^3/s, d_o = 0.119 m, Smooth PVC bed data

4. TURBULENT VELOCITY MEASUREMENTS

In a breaking bore, the turbulent velocity measurements showed that the arrival of the tidal bore and the sudden increase in water depth yielded a rapid flow deceleration. The longitudinal velocities showed a sudden deceleration at all vertical elevations. Some large fluctuations of the longitudinal, transverse and vertical velocity components were observed beneath the tidal bore. The front was followed by a highly turbulent flow motion with significant fluctuations of all velocity components. Some typical Eulerian measurements are presented in Figure 5 which shows the instantaneous free-surface elevation, longitudinal and vertical velocity components as function of time. An ensemble-median of each instantaneous velocity component was produced at selected vertical elevations. Some typical results are presented also in Figure 5 and compared with the instantaneous data for a experiment (Run 1).

Both the instantaneous and ensemble-averaged (EA) data showed some key features of the unsteady turbulence in breaking tidal bores. These included a rapid flow deceleration during the passage of the tidal bore roller above the sampling volume, some negative longitudinal velocity component next to the bed (Fig. 5) highlighting some transient recirculation "bubble". The experimental results showed that

the maximum horizontal velocity fluctuations occurred about the same time as when the maximum free-surface fluctuations were observed. The transverse velocity data V_y presented some large fluctuations after the bore front for $z/d_o \geq 0.43$, typically 5 to 10 times after the front passage, implying some intense secondary motion in the wake of the bore roller.

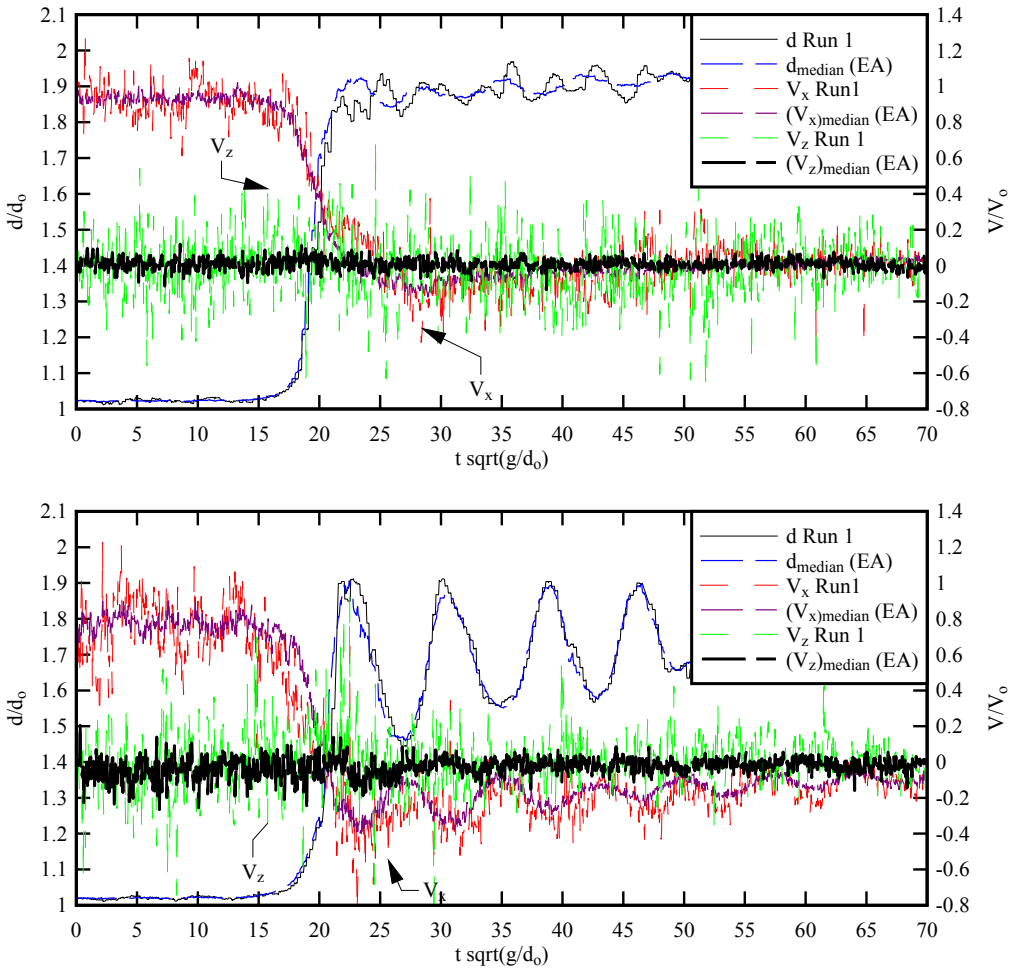

Figure 5 Free-surface and turbulent velocity measurements under a breaking tidal bore - Flow conditions: (A, Top) smooth PVC bed, Fr = 1.6, Re = 2.0×10^5, Q = 0.050 m^3/s, d_o = 0.118 m, z/d_o = 0.135; (B, Bottom) fixed gravel bed, Fr = 1.5, Re = 2.1×10^5, Q = 0.050 m^3/s, d_o = 0.126 m, z/d_o = 0.135

The vertical velocity data V_z presented a substantial positive value during the front passage for $z/d_o \geq 0.43$ (Docherty and Chanson 2010) that is believed to be closely linked with the streamline curvature immediately prior to the bore roller and possibly during the roller propagation. Since the free-surface is a streamline, the surface slope is related to the vertical velocity component at the free-surface:

$$\frac{V_z(z=d)}{V_x(z=d)} = \frac{\partial d}{\partial x} \quad (2)$$

where $V_x(z=d)$ is the horizontal velocity component at the surface while, at the bed, and $V_z(z=0) = 0$ for an impervious boundary. For a solitary wave, Boussinesq (1871) assumed a linear distribution of vertical velocity:

$$\frac{V_z}{V_z(z=d)} = \frac{z}{d} \quad (3)$$

The result may be applied to open channel flows with streamline curvature (Montes 1998). In the present study, the magnitude of the maximum median vertical velocity component $(V_z)_{max}$ increased with increasing distance from the bed. This is illustrated in Figure 6 showing the maximum median vertical velocity component as a function of the vertical elevation. On the same graph, the free-surface elevation rate $(\partial d/\partial t)_{z=d}$ is shown in addition. Since $V_z(z=0) = 0$ at the bed and $V_z(z=d) = (\partial d/\partial t)_{z=d}$ at the free-surface, an entire data trend can be extrapolated and the present data were best correlated by:

$$\left(\frac{V_z}{V_o}\right)_{max} = 0.215 \times \frac{z}{d_o} \qquad \textit{for } 0 < z/d < 1 \textit{ on smooth PVC} \quad (4a)$$

$$\left(\frac{V_z}{V_o}\right)_{max} = 0.466 \times \left(\frac{z}{d_o}\right)^{1.54} \qquad \textit{for } 0 < z/d < 1 \textit{ on fixed gravel} \quad (4b)$$

with a normalised correlation coefficient of 0.982 and 0.999 for Equations (4a) and (4b) respectively (Fig. 6). The smooth bed data (Eq. (4a)) corresponded to Boussinesq's (1871) approximation (Eq. (3)), and the gravel bed data yielded a similar monotonic relationship but with a different power law exponent (Eq. (4b)) & Fig. 6). The experimental results highlighted simply a quantitative difference between the smooth and rough bed, that might be associated with some effects of the bed roughness on the turbulent flow field, especially close to the bed.

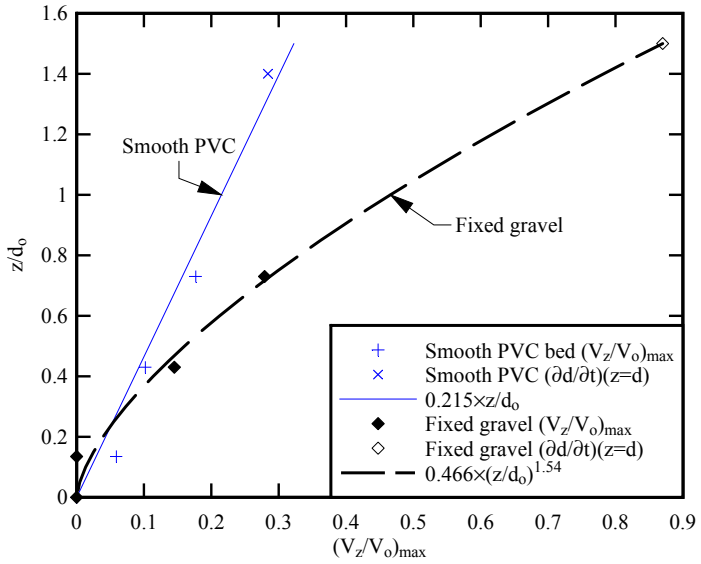

Figure 6 Maximum median vertical velocity beneath the tidal bore roller and corresponding free-surface vertical velocity on smooth PVC and fixed gravel beds - Comparison with Equations (4a) and (4b)

5. CONCLUSION

The turbulence and turbulent mixing in tidal bores was investigated physically under controlled conditions based upon an undistorted Froude similitude, with two types of bed roughness. Some free-surface measurements were conducted with both undular and breaking bores, and the tidal flow patterns were independent of the bed roughness. Using an ensemble-averaging technique, the free-surface fluctuations of breaking tidal bores were characterised. Immediately prior to the roller, the free-surface curved gradually upwards and the gentle surface elevation rise was about $0.1d_o$ where d_o is the initial water depth. The passage of the bore roller was associated with some large water depth fluctuations; the largest free-surface fluctuations were observed during the first half of the bore roller.

Some turbulent velocity measurements were performed at several vertical elevations during the breaking tidal bores. Both the instantaneous and ensemble-averaged velocity data highlighted some

basic features. A strong flow deceleration was observed at all vertical elevations and, close to the bed, the longitudinal velocity component became negative immediately after the roller passage, indicating a transient recirculation. The vertical velocity data showed some positive, upward motion during the bore passage with increasing maximum vertical velocity with increasing distance from the bed. The vertical motion was believed to be linked with some streamline curvature in front of the roller. The transverse velocity data presented some large fluctuations with non-zero ensemble-average after the roller passage that suggested some secondary turbulent motion advected behind the bore.

6. REFERENCES

Boussinesq, J.V. (1871). *Théorie de l'Intumescence appelée Onde Solitaire ou de Translation se Propageant dans un Canal Rectangulaire*. ('Theory of the Solitary Wave propagating in an Rectangular Channel.') Comptes-Rendus de l'Académie des Sciences, Paris, France, Vol. 72, pp. 755-759 (in French).

Chanson, H. (1999). *The Hydraulics of Open Channel Flow: An Introduction*. Edward Arnold, London, UK, 512 pages.

Chanson, H. (2010). *Unsteady Turbulence in Tidal Bores: Effects of Bed Roughness*. Journal of Waterway, Port, Coastal, and Ocean Engineering, ASCE, Vol. 136, No. 5, pp. 247-256 (DOI: 10.1061/(ASCE)WW.1943-5460.0000048).

Docherty, N.J., and Chanson, H. (2010). *Characterisation of Unsteady Turbulence in Breaking Tidal Bores including the Effects of Bed Roughness*. Hydraulic Model Report No. CH76/10, School of Civil Engineering, The University of Queensland, Brisbane, Australia, 112 pages.

Henderson, F.M. (1966). *Open Channel Flow. MacMillan Company*, New York, USA.

Hornung, H.G., Willert, C., and Turner, S. (1995). *The Flow Field Downstream of a Hydraulic Jump*. Jl of Fluid Mech., Vol. 287, pp. 299-316.

Koch, C., and Chanson, H. (2009). *Turbulence Measurements in Positive Surges and Bores*. Journal of Hydraulic Research, IAHR, Vol. 47, No. 1, pp. 29-40 (DOI: 10.3826/jhr.2009.2954).

Liggett, J.A. (1994). *Fluid Mechanics*. McGraw-Hill, New York, USA.

Montes, J.S. (1998). Hydraulics of Open Channel Flow. ASCE Press, New-York, USA, 697 pages.

Rayleigh, Lord (1908). *Note on Tidal Bores*. Proc. Royal Soc. of London, Series A containing Papers of a Mathematical and Physical Character, Vol. 81, No. 541, pp. 448-449.